Paper Type: Original Article

A New Generalized Inverse Rayleigh Geometric Distribution with Simulation and Applications in Medicine and Engineering

Adebisi Ade Ogunde[1,*] iD **, Innocent Osezuwa Oseghale[2]** iD **, Najeem Adesola Adeleye[3]** iD

[1] Department of Statistics, University of Ibadan, Oyo State, Nigeria; debiz95@yahoo.com.
[2] Department of Mathematics and Statistics, Federal University Otuoke, Bayelsa State; nnocentoseghale@gmail.com.
[3] Department of Statistics, Ogun State Institute of Technology, Igbesa, Ogun State; debiz95@yahoo.com.

Citation:

Abstract

Various limitations are inherent in existing statistical distributions, as explained in the literature when used in modeling the complexities of real-world data. This oftentimes brings about the development of new tractable models. This work introduces the new novel distribution named the Inverse Rayleigh Geometric (IRG) distribution. The IRG distribution boasts significant flexibility with symmetrical and asymmetrical shapes, allowing its Hazard Rate Function (HRF) to be adapted to many failure patterns experienced in various fields such as medicine, biology, and engineering. Some statistical properties of the IRG distribution, such as ordinary and incomplete moments, Quantile Function (QF), stress-strength reliability, weighted moments, order statistics, information measures, and Rényi and Tsallis entropies, are studied. A simulation study was carried out to evaluate the performance of the estimation method used. The IRG distribution proves to be superior to all other models considered in this study by its ability to fit real-life data accurately. Two medical and engineering datasets are applied to demonstrate the exceptional fit of the IRG distribution compared to competing models. The results indicate that the IRG distribution holds promise for reliability evaluations and lifetime data analysis in a variety of academic fields.

Keywords: Weighted moments, Stress-strength reliability, Tsallis entropy, Inverse Rayleigh distribution.

1 | Introduction

Treyer [1] introduced and developed the Inverse Rayleigh (IR) distribution as a model for analyzing reliability data. Voda [2] carried out an in-depth study on the model and discovered that the IR distribution is commonly used in reliability research and engineering, and it can be used to approximate different experimental units of lifespan distributions. Gharraph [3] derived five key measures of location for the IR distribution and used

various estimation methods to estimate the unknown parameter of this distribution. Further, He performed a numerical comparison of different estimating methods, concentrating on their bias and Root-Mean-Squared Error (RMSE), in order to assess the effectiveness and suitability of the recommended approach. Mukherjee and Maiti [4] proposed and studied the percentile estimator for the scale parameter λ of the one-parameter IR distribution and examined its asymptotic efficiency. In their study, Soliman et al. [5] examined both non-Bayesian and Bayesian problems pertaining to parameter estimation in the IR model.

Almarashi et al. [6] addressed issues with the IR distribution's two-parameter extension by utilizing the half logistic family to simulate somewhat positively-skewed or nearly symmetrical real-world data. The IR probability distribution is offered by Chiodo and Noia [7] as an alternate distribution for simulating extremely high wind speeds, which is essential for both mechanical safety evaluation and wind power generation. Importantly for wind power generation and turbine safety assessment, Chiodo et al. [8] further introduced the compound IR distribution as a model built for severe wind speeds. Bakoban and Al-Shehri [9] looked at the four-parameter lifetime model known as the beta inverse generalized IR distribution. They conducted a thorough analysis of the model's characteristics and applicability.

Further, several authors have also created and researched generalizations of the IR distribution with the goal of expanding its range of use in real-world data modeling. Such works include: Khan [10] developed the modified IR distribution and discussed its statistical properties. Khan and King [11] proposed and studied the transmuted modified IR distribution utilizing the Quadratic Rank Transmutation Map (QRTM). The Burr XII IR model was introduced by Goual and Yousof [12]. Fatima and Ahmad [13] developed the Weighted IR distribution. They carried out a detailed study of its statistical properties, which immensely contributes to the understanding and application of weighted distribution models in statistical analysis and applications. Exponentiated IR distribution features were investigated by Rao and Mbwambo [14], providing a versatile method for lifetime data analysis. The exponential transformed IR distribution was developed by Banerjee and Bhunia [15].

The development of new distributions usually entails the addition of one or more parameters to baseline distributions to enhance their applicability to model complex phenomena across various fields of life. Several authors have been motivated by this technique and have proposed different methods for generating new distributions. These include the Marshall and Olkin families of distribution developed by Marshall and Olkin [16]. The Beta Generalized distribution proposed by Eugene et al. [17], the Kumaraswamy Generalized distribution by Cordeiro and Castro [18], the McDonald Generalized distribution by Alexander et al. [19], and Shaw and Buckley [20] developed the transmuted Generalized families of distributions. Type II Topp-Leone generalized distribution was studied by Eligahy et al. [21], Alzaatreh and Ghosh [22] developed the Weibull X generalized distributions, the odd-generalized exponential-G was proposed by Tahir et al. [23], and Poisson odd-generalized exponential-G by Muhammad [24]. The Transmuted Generalized Poisson distribution by Yousof et al. [25], Sin Kumaraswamy generalized distribution, and Sin Topp-Leone generalized distribution were respectively studied by Jamal and Chesneau [26] and Al-Babtain et al [27] among several others. This work focuses on extending the one-parameter IR distribution to address the problem of monotone failure rate embedded in the IR distribution, which makes it inappropriate for use in modeling real-life data with a non-monotone hazard failure rate due to a problem associated with its tail weight.

1.1 | Motivation of Study

The chief motivation of this article is to develop a new generalization of the IR distribution called the Inverse Rayleigh Geometric (IRG) distribution. The relevance of the IRG distribution and its desirable properties include the following:

I. The density and Hazard Rate Functions (HRFs)' features and application of the **IRG** model will be enhanced, which will also better represent the behavior of a number of real-world occurrences. There are other forms that the HRF of the **IRG** distribution might take, such as increasing, decreasing, and inverted bathtub failure

rate. The density can take symmetrical and asymmetrical shapes. This will enable the IRG model to fit a wide range of data from the engineering, medicine, and reliability fields.

II. The IRG introduces new generalizations of the IR distribution by adding a new parameter, thus increasing its flexibility and improving its ability to characterize tail shapes more accurately as observed from the different shapes of the IRG density and hazard functions. Therefore, this generalization will help the IR's inability to fit real-world data that possesses a non-monotone failure rate.

III. The Cumulative Distribution Function (CDF) and HRFs, moments, and entropy of the IRG are in closed forms, which are helpful in analyzing complete and censored data.

The rest of the paper is organized as follows: we derived an expression for the distribution and density functions, reliability properties, expansions of the Probability Density Function (PDF), Quantile Function (QF), and mode, and also studied the nature of Skewness and Kurtosis of the new distribution in Section 2. In Section 3, some statistical properties of the IRG distribution are examined. The maximum likelihood method used in estimating the parameters of the IRG model in Section 4 is presented to estimate the model parameters. A simulation study is performed in Section 5. In Section 6, we illustrate the flexibility of the new model using two real data sets. Some concluding remarks are offered in Section 7.

2 | Methodology

If there exists Q functional component of a system working in series and operating independently from each other. Suppose each component failure time is denoted by $Z_1, \ldots, Z_Q$ and the system stops functioning when one of the components fails. Suppose the failure time of the components Z follows the IR distribution with CDF represented by

$$G(x; \rho) = \exp\left(-\frac{\rho}{x^2}\right), \qquad x > 0; \rho > 0. \tag{1}$$

The associated PDF to *Eq. (1)* is

$$g(x; \rho) = \frac{2\rho}{x^3} \exp\left(-\frac{\rho}{x^2}\right), \qquad x > 0; \rho > 0. \tag{2}$$

And Q is a discrete random variable having a geometric distribution with probability function $p(n; p) = (1 - p)p^{n-1}$ for $n\epsilon N$ and $p\epsilon(0,1)$. Let $X = \min\{z_i\}_{i=1}^N$. The marginal PDF of X is

$$f(x; \rho, v) = (1 - v)\frac{2\rho}{x^3} \exp\left(-\frac{\rho}{x^2}\right)\left[1 - v\left(1 - \exp\left(-\frac{\rho}{x^2}\right)\right)\right]^{-2}. \tag{3}$$

The corresponding CDF is

$$F(x; \rho, v) = \frac{\exp\left(-\frac{\rho}{x^2}\right)}{\left[1 - v\left(1 - \exp\left(-\frac{\rho}{x^2}\right)\right)\right]}. \tag{4}$$

Where ρ is the scale parameter and v is a shape parameter. The functional reliability properties of the IRG distribution are presented below. The Survival Function (SF), HRF, Cumulative Hazard Rate Function (CHRF), and the Reversed Hazard Rate Function (RHRF) are given, respectively, by

$$s(x; \rho, v) = 1 - \frac{\exp\left(-\frac{\rho}{x^2}\right)}{\left[1 - v\left(1 - \exp\left(-\frac{\rho}{x^2}\right)\right)\right]}. \tag{5}$$

$$h(x; \rho, v) = \frac{(1-v)\frac{2\rho}{x^3}\exp\left(-\frac{\rho}{x^2}\right)\left[1 - v\left(1 - \exp\left(-\frac{\rho}{x^2}\right)\right)\right]^{-1}}{1 - v + (v-1)\exp\left(-\frac{\rho}{x^2}\right)}. \tag{6}$$

$$\varsigma(x; \rho, v) = \frac{(1-v)\frac{2\rho}{x^3}}{\left[1 - v\left(1 - \exp\left(-\frac{\rho}{x^2}\right)\right)\right]}. \tag{7}$$

And

$$H(x; \rho, v) = \left(-\frac{\rho}{x^2}\right) + \log\left[1 - v\left(1 - \exp\left(-\frac{\rho}{x^2}\right)\right)\right], \tag{8}$$

Figs. 1-5 show the variability in the shapes of the CDF, PDF, S(x), and h(x) for the IRG distribution. From *Fig. 1*, it can be concluded that the distribution function of the IRG function has a proper density function. *Fig. 2* and *Fig. 3* show that the PDF of the IRG distribution displays shapes with increasing, decreasing, and unimodal patterns. From *Fig. 4*, we observe that as time increases, the survival probability approaches zero, that is, it decreases. *Fig. 5* demonstrates that the HRF of the IRG distribution showcases patterns marked with increasing, decreasing, and inverted bathtub failure rate.
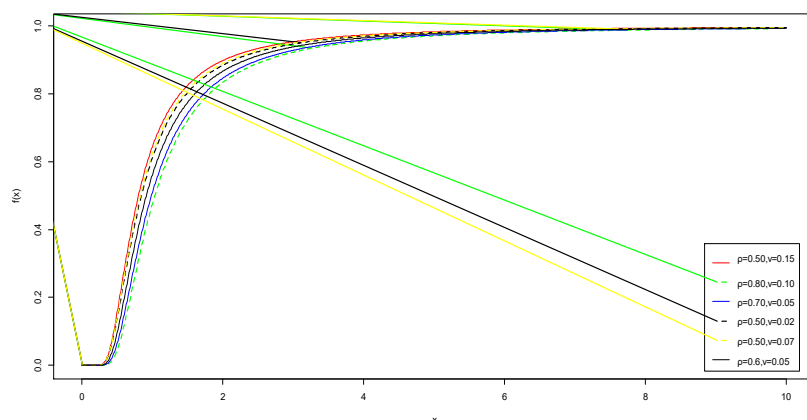
Fig. 1. The cumulative distribution functions of the inverse Rayleigh geometric distribution.
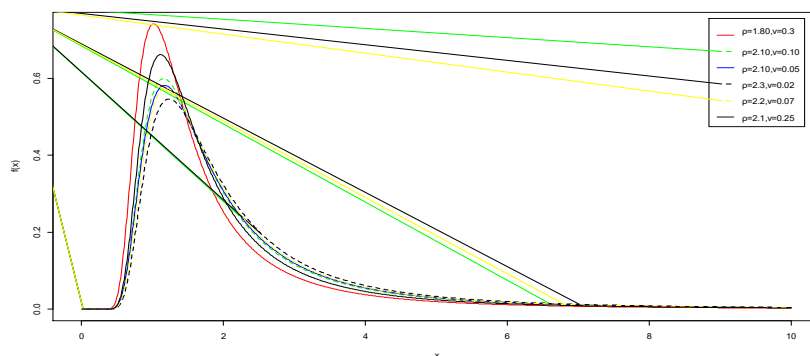
Fig. 2. The probability density functions of the inverse Rayleigh geometric distribution.
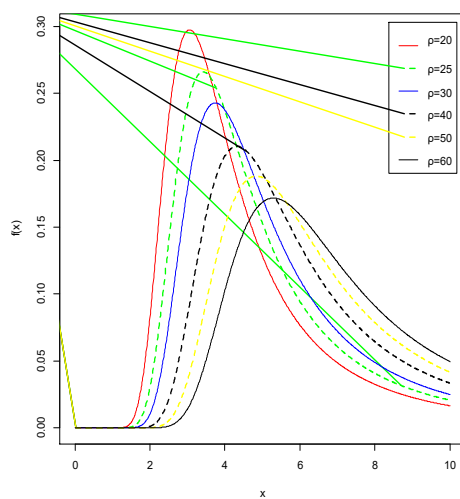
a.
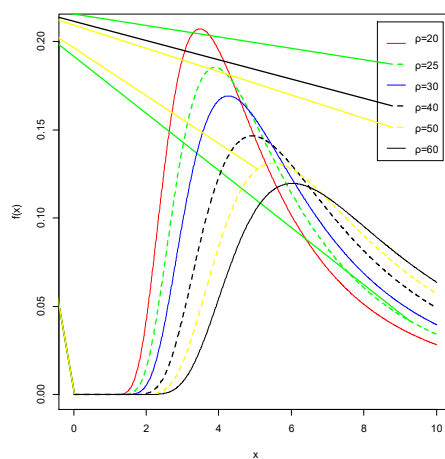
b.

Fig. 3. The probability density functions of the inverse Rayleigh geometric distribution; a. density function of inverse Rayleigh geometric distribution, v=0.6 and b. density function of inverse Rayleigh geometric distribution, v=0.2.
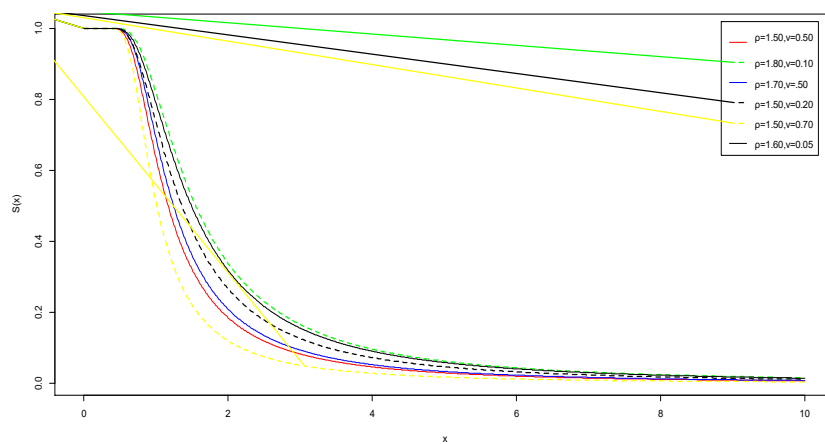
Fig. 4. The survival function of inverse Rayleigh geometric distribution.

A new generalized inverse Rayleigh geometric distribution with simulation and ...

230
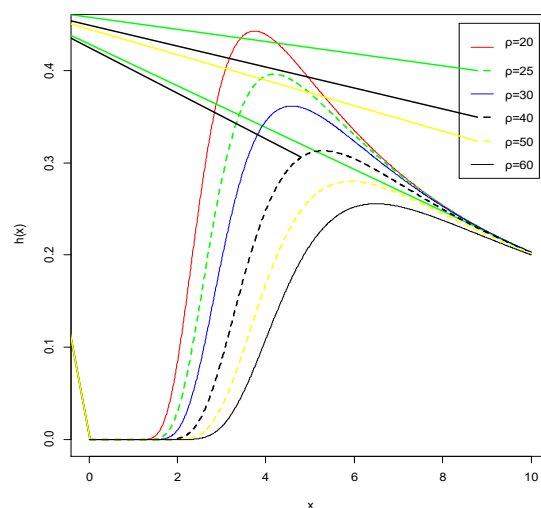
a.
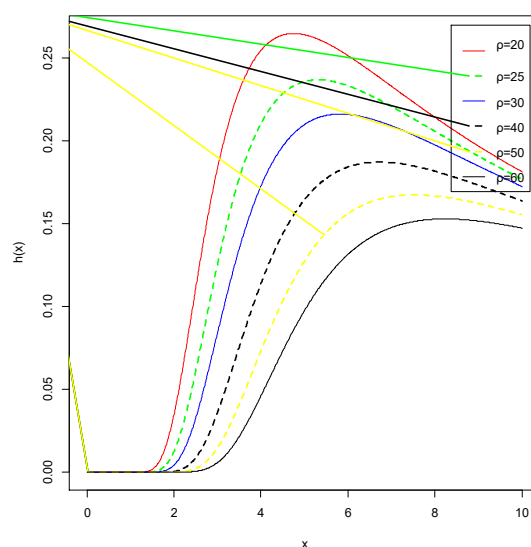
b.

Fig. 5. The hazard rate function of the inverse Rayleigh geometric distribution;
a. Hazard function of inverse Rayleigh geometric distribution, v=0.6 and b.
Hazard function of inverse Rayleigh geometric distribution, v=0.2.

2.1 | Expansion of the Density Function

In this subsection, we can write the Generalized IR distribution as an infinite mixture of the IR distribution. If $|m| < 1, u > 0$, and $w > 0$, we have the series representation

$$(1 - m)^{-u} = \sum_{i=0}^{\infty} \binom{u + i - 1}{i} m^i.$$

(9)

And

$$(1 - m)^{f-1} = \sum_{i=0}^{\infty} (-1)^i \binom{f - 1}{i} m^i.$$

(10)

Expanding $\left[1 - v\left(1 - \exp\left(-\frac{\rho}{x^2}\right)\right)\right]^{-2}$ using *Eq. (9)* and *Eq. (10)*, finally, we have

$$f(x; \rho, v) = 2(1 - v)\rho \sum_{i=j=0}^{\infty} v^i(-1)^j \binom{i+1}{i}\binom{j}{i} x^{-3} e^{-(j+1)\frac{\rho}{x^2}} = \sum_{i=0}^{\infty} \gamma_j f(x; (j+1)\rho), \tag{11}$$

where,

$$\gamma_j = 2(1 - v)\rho \sum_{i=j=0}^{\infty} v^i(-1)^j \binom{i+1}{i}\binom{j}{i}.$$

And $f(x; (j + 1)\rho)$ denotes the IR density function with parameter $(j + 1)\rho$. Thus, the IRG density function can be written as an infinite linear combination of IR densities, and then some of its basic mathematical and statistical properties can be derived from IR properties.

2.2 | Quantile of Inverse Rayleigh Geometric Distribution

The inverse of the CDF in *Eq. (4)* gives the QF of the IRG distribution as

$$Q_{(u)} = \left[-\frac{1}{\rho}\left(\log\left[\frac{u(1-v)}{(1-uv)}\right]\right)\right]^{-1/2}, \qquad u\epsilon(0,1). \tag{12}$$

The expression given *Eq. (12)* is very useful to generate IRG random variates, which can easily be implemented using software. In particular, an expression for the median (M) of X is Q (0.5) given by

$$M = Q_{(0.5)} = \left[-\frac{1}{\rho}\left(\log\left[\frac{0.5(1-v)}{(1-0.5v)}\right]\right)\right]^{-1/2}. \tag{13}$$

2.3 | Mode

For a continuous random variable with PDF f(x), the mode is defined as the value at which f(x) reaches its maximum value. The mode of the inverse generalized Rayleigh distribution can be estimated by finding a solution to the equation $\frac{\partial y}{\partial x}(\log[f(x; \rho, v]) = 0$.

$$\frac{\partial y}{\partial x}(\log[f(x; \rho, v]) = -\frac{3}{x} + \frac{2\rho}{x^3} + \frac{4v\exp\left(-\frac{\rho}{x^2}\right)}{x^3\left[1 - v\left(1 - \exp\left(-\frac{\rho}{x^2}\right)\right)\right]} = 0.$$

2.4 | Skewness and Kurtosis Based on the Quantile Function

Now we consider the analytical expression for Skewness and Kurtosis of the IRG distribution by using the QF given in *Eq. (13)*. Suppose $Q_{(u)} = Q(u; \varphi)$ with $u\epsilon(0,1)$. Thus, we consider the Galton coefficient of Skewness (SK) by Galton [28] and the coefficient of Kurtosis (KK) by Moors [29], respectively, designed using the QF. The Galton's Skewness and Moors' Kurtosis are defined by

$$GSK = \frac{Q_{3/4} - 2Q_{1/2} + Q_{1/4}}{Q_{3/4} - Q_{1/4}}, \qquad MK = \frac{Q_{7/8} - Q_{5/8} + Q_{3/8} - Q_{1/8}}{Q_{6/8} - Q_{2/8}},$$

respectively. Here, GSK measures the degree of asymmetry of the IRG distribution, and MK measures the degree of its tail heaviness; as the value of MK increases, the tail of the IRG distribution becomes heavier. *Tables 1-3* displays some basic characteristics of the IRG model. From *Table 1* and *Table 2*, it can be deduced that increasing the values of the parameter ρ while keeping the value of parameter v constant will lead to an increase in the values of the Lower quartile ($Q_{1/4}$), middle quartile ($Q_{1/2}$), and the upper quartile ($Q_{3/4}$) while keeping the values of the Galton Skewness and Moors Kurtosis constant. *Table 3* shows that varying the values of parameters ρ and v will cause the values of the Galton coefficient of Skewness and Moors coefficient of Kurtosis to increase and decrease as the values become larger.

Table 1. Quartiles, Skewness of inverse Rayleigh geometric distribution for v = 0.2.

	$Q_{1/4}$	$Q_{1/2}$	$Q_{3/4}$	$Q_{1/8}$	$Q_{3/8}$	$Q_{5/8}$	$Q_{7/8}$	GSK	MK
ρ =0.5	0.5665	0.7852	1.1981	0.4686	0.6664	0.9452	1.7445	0.3074	1.5784
ρ =1.5	0.9812	1.3601	2.0752	0.8116	1.1542	1.6372	3.0215	0.3074	1.5784
ρ =5	1.7914	2.4831	3.7888	1.4818	2.1078	2.9891	5.5164	0.3074	1.5784
ρ =10	2.5334	3.5116	5.3582	2.0955	2.9801	4.2272	7.8014	0.3074	1.5784
ρ =20	3.5827	4.9662	7.5776	2.96353	4.2145	5.9782	11.0330	0.3074	1.5784
ρ =30	4.3879	6.08	9.2807	3.6296	5.1617	7.3218	13.5126	0.3074	1.5784

Table 2. Quartiles, Skewness of inverse Rayleigh geometric distribution for v = 0.8.

	$Q_{1/4}$	$Q_{1/2}$	$Q_{3/4}$	$Q_{1/8}$	$Q_{3/8}$	$Q_{5/8}$	$Q_{7/8}$	GSK	MK
ρ=0.5	0.4247	0.5282	0.7140	0.3735	0.4731	0.6006	0.9632	0.2839	1.5975
ρ=1.5	0.7355	0.9150	1.2367	0.6469	0.8195	10402	1.6682	0.2839	1.5975
ρ =5	1.3429	1.6705	2.2578	1.1812	1.4962	1.8991	3.0457	0.2839	1.5975
ρ=10	1.8991	2.3624	3.1930	1.6705	2.1159	2.6858	4.3073	0.2839	1.5975
ρ=20	2.6858	3.3410	4.5156	2.3624	2.9924	3.7983	6.0915	0.2839	1.5975
ρ=30	3.2894	4.0919	5.5305	2.8934	3.6649	4.6519	7.4605	0.2839	1.5675

Table 3. Quartiles, Skewness of inverse Rayleigh geometric distribution.

	$Q_{1/4}$	$Q_{1/2}$	$Q_{3/4}$	$Q_{1/8}$	$Q_{3/8}$	$Q_{5/8}$	$Q_{7/8}$	GSK	MK
ρ = 10 v = 0.1	2.6115	3.6583	5.6336	2.1456	3.0891	4.4245	8.2388	0.3072	1.5742
ρ = 15 v = 0.4	3.9107	3.9107	5.8266	2.4306	3.3594	4.6519	8.3805	0.3064	1.5878
ρ = 25 v = 0.5	3.5843	4.7703	6.9957	3.0384	4.1291	5.6309	9.9738	0.3047	1.5928
ρ = 30 v = 0.6	3.7441	4.8936	7.0351	3.2065	4.2741	5.7220	9.9115	0.3015	1.5974
ρ = 40 v = 0.7	4.0843	5.2229	7.3166	3.5401	4.6123	6.0340	10.1343	0.2955	1.6003
ρ = 50 v = 0.9	3.8158	4.5664	5.8394	3.4249	4.1727	5.0690	7.5067	0.2582	1.5742

3 | Moments and Incomplete Moments of Inverse Rayleigh Geometric Distribution

Theorem 1. Let X be a random variable following an IRG distribution with shape parameters v and ρ. The rth moment about the origin of X, represented by $E(X^r)$, gives as:

$$E(X^r) = \mu'_r = (1 - v) \sum_{i=j=0}^{\infty} (i + 1)(-1)^j v^i (j + 1)^{r/2 - 1} \binom{j}{i} \rho^{r/2} \Gamma\left(1 - r/2\right), r < 2. \tag{14}$$

Proof:

$$E(X^r) = \int_0^{\infty} x^r f(x; \phi)\, dx = 2\rho \sum_{2i=j=0}^{\infty} v^i (-1)^j (1 - v) \binom{i + 1}{i} \binom{j}{i} \int_{-\infty}^{\infty} x^{r-3} e^{-(j+1)\frac{\rho}{x^2}}\, dx, \tag{15}$$

Letting $z = (j + 1)\frac{\rho}{x^2}$, $x = z^{-1/2}(j + 1)^{1/2}\rho^{1/2}$, $dx = -1/2\, z^{-3/2}(j + 1)^{1/2}\rho^{1/2}$, inserting it in *Eq. (15)*, we obtain

$$E(X^r) = \mu'_r = (1 - v) \sum_{2i=j=0}^{\infty} (i + 1)v^i(-1)^j(j + 1)^{r/2-1} \binom{j}{i} \rho^{r/2} \int_0^{\infty} z^{-r/2}e^{-z} \, dz. \tag{16}$$

$$\mu'_r = (1 - v) \sum_{i=j=0}^{\infty} (i + 1)(-1)^j v^i(j + 1)^{r/2-1} \binom{j}{i} \rho^{r/2}\Gamma\left(1 - \frac{r}{2}\right), \qquad r < 2, \tag{17}$$

where $\Gamma(m) = \int_0^{\infty} u^{m-1}e^{-u}du$ is the complementary incomplete gamma function. The mean of IRG can be obtained by substituting $r = 1$ in *Eq. (17)*, and is given as

$$\text{mean} = \mu = (1 - v) \sum_{i=j=0}^{\infty} (i + 1)(-1)^j v^i(j + 1)^{-1/2} \binom{j}{i} \rho^{1/2}\Gamma\left(\frac{1}{2}\right). \tag{18}$$

The qth central moment (M_q) and cumulants (k_q) of X, are respectively, given by

$$M_q = E\left(X - \mu'_q\right)^q = \sum_{p=0}^{q-1} \binom{q - 1}{p - 1} k_r \mu'_{q-r,}$$

and

$$k_r = \mu'_r - \sum_{p=0}^{q-1} \binom{q - 1}{p - 1} k_r \mu'_{q-r,}$$

where $k_1 = \mu'_1$.

Theorem 2. If $X \sim$ IRG, then an expression for the Moment Generating Function (MGF) of X is given as

$$M_x(t) = (1 - v) \sum_{i=j=0}^{\infty} \frac{t^r}{r!}(i + 1)(-1)^j v^i(j + 1)^{r/2-1} \binom{j}{i} \rho^{r/2}\Gamma\left(1 - \frac{r}{2}\right).$$

Proof: From the well-known definition of the MGF given by

$$M_x(t) = E(e^{tX}) = \sum_{r=0}^{\infty} \frac{t^r}{r!} \int_{-\infty}^{\infty} x^r f(x)dx = \sum_{r=0}^{\infty} \frac{t^r}{r!} \mu'_r.$$

Substituting *Eq. (17)* in *Eq. (19)* for μ'_r, we obtain the MGF of the IRG distribution as

$$M_x(t) = (1 - v) \sum_{i=j=0}^{\infty} \frac{t^r}{r!}(i + 1)(-1)^j v^i(j + 1)^{r/2-1} \binom{j}{i} \rho^{r/2}\Gamma\left(1 - \frac{r}{2}\right).$$

The rth lower incomplete moments of X are defined by

$$Л_r(t) = \int_{-\infty}^{t} x^r f(x; \phi) \, dx. \tag{20}$$

Inserting *Eq. (3)* in *Eq. (20)*, we obtain

$$Л_r(t) = 2\rho \sum_{2i=j=0}^{\infty} v^i(-1)^j(1 - v) \binom{i + 1}{i} \binom{j}{i} \int_{-\infty}^{t} x^{r-3}e^{-(j+1)\frac{\rho}{x^2}} \, dx, \tag{21}$$

Letting $z = (j + 1)\frac{\rho}{x^2}$, $x = z^{-1/2}(j + 1)^{1/2}\rho^{1/2}$, $dx = \frac{-1}{2} z^{-3/2}(j + 1)^{1/2}\rho^{1/2}$, inserting it in *Eq. (21)*, we obtain

$$Л_r(t) = (1 - v) \sum_{2i=j=0}^{\infty} (i + 1)v^i(-1)^j(j + 1)^{r/2-1} \binom{j}{i} \rho^{r/2} \int_0^{t} z^{-r/2}e^{-z} \, dz. \tag{22}$$

Finally, we obtain

$$Л_r(t) = (1 - v) \sum_{i=j=0}^{\infty} (i + 1)(-1)^j v^i (j + 1)^{r/2-1} \binom{j}{i} \rho^{r/2} \gamma \left(1 - \frac{r}{2}, (j + 1)\frac{\rho}{t^2}\right), \tag{23}$$

where $\gamma(m, n) = \int_0^{\infty} y^{n-1} e^{-y} dy - \int_m^{\infty} y^{n-1} e^{-y} dy = \int_0^a y^{n-1} e^{-y} dy$ is the incomplete gamma function. The first incomplete moment is given as

$$Л_1(t) = (1 - v) \sum_{i=j=0}^{\infty} (i + 1)(-1)^j v^i (j + 1)^{-1/2} \binom{j}{i} \rho^{1/2} \Gamma \left(\frac{1}{2}, (j + 1)\frac{\rho}{t^2}\right). \tag{24}$$

It should be noted that *Eq. (24)* is a very important quantity in deriving an expression for both the Lorenz and Bonferroni curves.

3.1 | Mean Deviation

In this subsection, we derive an expression for the mean deviation about the mean and the mean deviation about the median. If X has the IRG distribution, then we can compute the mean deviations about the mean $\mu = E(X)$ and the mean deviations about the median M as

$$\delta_1(x) = \int_0^{\infty} |x - \mu| f(x) dx = 2[\mu f(\mu) - q(\mu)], \tag{25}$$

and

$$\delta_1(x) = \int_0^{\infty} |x - M| f(x) dx = \mu - 2Q(M), \tag{26}$$

respectively. the measures $\delta_1(x)$ and $\delta_2(x)$ can be estimated using the relationship $q(.)$ as

$$q(v) = \int_0^v x f(x) dx = (1 - v) \sum_{i=j=0}^{\infty} (i + 1)(-1)^j v^i (j + 1)^{-1/2} \binom{j}{i} \rho^{1/2} \Gamma \left(\frac{1}{2}, (j + 1)\frac{\rho}{v^2}\right).$$

3.2 | Bonferroni and Lorenz Curves

Measures of income inequality, such as the Lorenz and Bonferroni curves, are helpful in various domains such as insurance, demography, reliability, and medicine. The Lorenz curve for a positive random variable X is defined as

$$L_T = \frac{1}{\mu} \int_0^x x f(x) dx = \frac{Л_1(t)}{\mu} = \frac{(1 - v) \sum_{i=j=0}^{\infty} (i + 1)(-1)^j v^i (j + 1)^{-1/2} \binom{j}{i} \rho^{1/2} \Gamma \left(\frac{1}{2}, (j + 1)\frac{\rho}{t^2}\right)}{\mu}. \tag{27}$$

And

$$B_T = \frac{L_T}{t} = \frac{(1 - v) \sum_{i=j=0}^{\infty} (i + 1)(-1)^j v^i (j + 1)^{-1/2} \binom{j}{i} \rho^{1/2} \Gamma \left(\frac{1}{2}, (j + 1)\frac{\rho}{t^2}\right)}{t\mu}. \tag{28}$$

3.3 | Residual Life and Reversed Residual Life Functions

Assume that a part survives for a certain amount of time $t > 0$, the residual life is the period that exceeds t until the time when failure is observed and is defined by the conditional random variable $X - t|X > t$. In reliability theory, it has been established that the mean residual life function and the ratio of two consecutive moments of residual life can be used to determine the distribution uniquely. Therefore, we obtain the sth order moment of the residual life via the general formula given by

$$mrl(t) = E[(X - t)^s/X > t] = \frac{1}{S_{IRG}(t)} \int_0^t (x - t)^s f(x) dx. \tag{29}$$

Using the binomial expansion for $(x - t)^s$ and substituting $f(x, \varphi)$ given by *Eq. (3)* into *Eq. (29)* finally gives

$$mrl(t) = \frac{(1 - v)}{S_{IRG}(t)} \sum_{i=j=l=0}^{\infty} \frac{(i + 1)(-1)^{s+j-l} s! \, t^{s-l} v^i}{l! \, \Gamma(s - l + 1)} (j + 1)^{\frac{r}{2}-1} \binom{j}{i} \rho^{\frac{r}{2}} \gamma \left(1 - \frac{r}{2}, (j + 1) \frac{\rho}{t^2}\right).$$

Consequently, the sth moment of the residual life of X can be derived as

$$MRL(t) = E[(t - X)^s/X > t] = \frac{1}{F_{IRG}(t)} \int_0^t (x - t)^s f(x) dx. \tag{30}$$

The sth moment of the reversed life of X

$$MRL(t) = \frac{(1 - v)}{F_{IRG}(t)} \sum_{i=j=l=0}^{\infty} \frac{(i + 1)(-1)^{l+j} s! \, v^i}{l! \, \Gamma(s - l)!} (j + 1)^{\frac{r}{2}-1} \binom{j}{i} \rho^{\frac{r}{2}} \gamma \left(1 - \frac{r}{2}, (j + 1) \frac{\rho}{t^2}\right).$$

3.4 | Probability Weighted Moment

The $(r, s)^{th}$ PWM OF x represented by X is statistically defined by

$$\mu_{r,s} = E\{X^r G(X)^s\} = \int_{-\infty}^{\infty} x^r G(X)^s g(x) dx. \tag{31}$$

Inserting *Eq. (3)* and *Eq. (4)* into *Eq. (31)*, followed by further simplification using *Eq. (10)*, we obtain

$$\mu_{r,s} = 2\rho(1 - v) \sum_{p=q=0}^{\infty} (-1)^q \binom{s + p + 1}{p} \binom{q}{p} v^p \int_{-\infty}^{\infty} x^{-3} e^{-(s+q+1)\frac{\rho}{x^2}} dx, \tag{32}$$

By taking $m = (s + q + 1)\frac{\rho}{x^2}$, $x = m^{-1/2}(s + q + 1)^{1/2}\rho^{1/2}$, and

$dx = -2^{-1/2}m^{-3/2}(s + q + 1)^{1/2}\rho^{1/2}dm$, and substitute it in *Eq. (32)*, we have

$$\mu_{r,s} = (1 - v) \sum_{p=q=0}^{\infty} (-1)^q \binom{s+p+1}{p} \binom{q}{p} v^p \rho^{r/2}(s + q + 1)^{(r/2-1)} \int_{-\infty}^{\infty} m^{-r/2} e^{-m} dm, \tag{33}$$

Finally, we have an expression for the probability weighted moments as

$$\mu_{r,s} = (1 - v) \sum_{p=q=0}^{\infty} (-1)^q \binom{s + p + 1}{p} \binom{q}{p} v^p \rho^{r/2}(s + q + 1)^{(r/2-1)} \Gamma\left(1 - \frac{r}{2}\right).$$

3.5 | Stress-Strength Reliability

Suppose a system has h components that are identical, of which j components are functioning. The strength of the h components is X_1, with common CDF $F(x; \rho, v_1)$ while the stress Y_2 imposed on the components has CDF $F(x; \rho, v_2)$. The strength $X_i, i = 1,2, \dots, h$ and stress Y_2 are $i.i.d.$ the reliability that the system functions properly is given by

$$\Re = P(Y_2 < X_1) = \int_{-\infty}^{\infty} f_1(x; \rho, v_1) F_2(x; \rho, v_2) dx, \tag{34}$$

If $X \sim IRG(\varphi)$, then $\Re$ is given by

$$\mathfrak{K} = (1 - v_1) \sum_{i=j=k}^{\infty} (i + 1) \binom{j}{i} (-1)^{j+1} \binom{l}{k} v_1^i v_2^k (j + l + 1)^{-1}. \tag{34}$$

3.6 | Rényi and Tsallis Entropy

Entropy measures the degree of variation in the level of uncertainty in a given system. Here, we consider the two essential types of entropy known as the Rényi and Tsallis entropies. The Rényi entropy measure of a random variable X with an IRG distribution can be defined by

$$I_\zeta(\phi) = \frac{1}{1 - \zeta} \log \left[\int_0^\infty f(x; \phi)^\zeta \, dx \right], \qquad \zeta \neq 1 \text{ and } \zeta > 0. \tag{35}$$

Plugging *Eq. (3)* in *Eq. (35)*, we obtain

$$I_\zeta(\phi) = \frac{1}{1 - \zeta} \log \left[\int_0^\infty \left((1 - v) \frac{2\rho}{x^3} \exp\left(-\frac{\rho}{x^2}\right) \left[1 - v \left(1 - \exp\left(-\frac{\rho}{x^2}\right) \right) \right]^{-2} \right)^\zeta dx \right], \tag{36}$$

Using the series expansion given in *Eq. (10)*, we obtain

$$I_\zeta(\phi) = \frac{1}{1 - \zeta} \log \left[(1 - v)^\zeta 2^{\zeta-1} \rho^{\frac{(1-\zeta)}{2}} \sum_{k=0}^{\infty} \sum_{l=0}^{k} M_{l,k} \right], \tag{37}$$

where, $M_{l,k} = \binom{2\zeta+k-1}{k} \binom{l}{k} (-1)^l v^k (l + 1)^{\frac{1-3\zeta}{2}} \Gamma\left(1 + \frac{3(\zeta-1)}{2}\right)$.

3.6.1 | Tsallis entropy

Tsallis entropy was developed by Tsallis [30], and its mathematical representation is given by

$$I_T^{(\zeta)} = \frac{1}{\zeta - 1} \left[1 - \int_0^\infty g_{IRG}(x)^\zeta \right], \quad \zeta > 0, \zeta \neq 1. \tag{38}$$

Since,

$$\int_0^\infty g(x)^\zeta = (1 - v)^\zeta 2^{\zeta-1} \rho^{\frac{(1-\zeta)}{2}} \sum_{k=0}^{\infty} \sum_{l=0}^{k} M_{l,k}.$$

Therefore,

$$I_T^{(\zeta)} = \frac{1}{\zeta - 1} \left[1 - (1 - v)^\zeta 2^{\zeta-1} \rho^{\frac{(1-\zeta)}{2}} \sum_{k=0}^{\infty} \sum_{l=0}^{k} M_{l,k} \right]. \tag{39}$$

3.7 | Order Statistics

Suppose $X_1, X_2, X_3, X_4, \dots, X_5$ represent an ordered random variable from the IRG distribution, then the PDF of the jth order statistic is given by

$$f_{(j,n)(x)} = \frac{n!}{(j - 1)! \, (n - j)!} f(x) F(x)^{(j-1)} \{1 - F(x)\}^{n-j}, \tag{40}$$

Using *Eq. (3)* and *Eq. (4)*, the maximum and the minimum order statistic of the IRG distribution are, respectively, given by

$$f_{(n,n)(x)} = n(1-v)\frac{2\rho}{x^3}\exp\left(-\frac{\rho}{x^2}\right)\left[1-v\left(1-\exp\left(-\frac{\rho}{x^2}\right)\right)\right]^{-2} \times \left(\frac{\exp\left(-\frac{\rho}{x^2}\right)}{\left[1-v\left(1-\exp\left(-\frac{\rho}{x^2}\right)\right)\right]}\right)^{n-1}, \quad (41)$$

and

$$f_{(1,n)(x)} = n(1-v)\frac{2\rho}{x^3}\exp\left(-\frac{\rho}{x^2}\right)\left[1-v\left(1-\exp\left(-\frac{\rho}{x^2}\right)\right)\right]^{-2} \times \left\{1-\frac{\exp\left(-\frac{\rho}{x^2}\right)}{\left[1-v\left(1-\exp\left(-\frac{\rho}{x^2}\right)\right)\right]}\right\}^{n-1}. \quad (42)$$

4 | Maximum Likelihood Estimation of Inverse Rayleigh Geometric Model

Let $x_1, x_2, \ldots, x_n$ be a random sample of size n drawn from IRG(ϕ), let $\phi = (\rho, v)^T$ represent the parameter vector. The likelihood function is defined

$$L = \prod_{i=1}^{n} f(x; \rho, v), \quad (43)$$

The log likelihood function for the vector of parameters is given as

$$\log L = n\log(1-v) + n\log(2\rho) - 3\sum_{i=1}^{n}\log(x_i) - \rho\sum_{i=1}^{n}x_i^{-2} - 2\sum_{i=1}^{n}\left[1-v\left(1-\exp\left(-\frac{\rho}{x_i^2}\right)\right)\right]. \quad (44)$$

The above log-likelihood expression in *Eq. (44)* can be maximized numerically by SAS or the Ox program, among many others. The associated score function is given by $U_n(\phi) = (\frac{\partial \log L}{\partial \rho}, \frac{\partial \log L}{\partial v})^T$.

The log-likelihood can be maximized by providing a numerical solution to the nonlinear likelihood equations obtained by differentiating *Eq. (44)*. The components of the score vector are represented by

$$\frac{\partial \log L}{\partial \rho} = \frac{n}{\rho} - \sum_{i=1}^{n}x_i^{-2} + 2v\sum_{i=1}^{n}\frac{x_i^{-2}e^{\left(-\frac{\rho}{x_i^2}\right)}}{\left[1-v\left(1-e^{\left(-\frac{\rho}{x_i^2}\right)}\right)\right]}. \quad (45)$$

$$\frac{\partial \log L}{\partial v} = 2v\sum_{i=1}^{n}\frac{\left(1-e^{\left(-\frac{\rho}{x_i^2}\right)}\right)}{\left[1-v\left(1-e^{\left(-\frac{\rho}{x_i^2}\right)}\right)\right]} - \frac{n}{1-v}. \quad (46)$$

The Maximum Likelihood Estimation (MLE) of ϕ, say $\hat{\phi}$, is obtained by proving a solution to the nonlinear system $U_n(\phi) = 0$. The solutions to these equations cannot be obtained analytically; nevertheless, they can be quantitatively solved using iterative techniques using statistical software. We need the information matrix for hypothesis testing on the model parameters and interval estimation. The three-by-three observed information matrix is provided by

$$U_n(\phi) = -\begin{vmatrix} U_{\rho\rho} & U_{\rho v} \\ U_{v\rho} & U_{vv} \end{vmatrix}.$$

and $U_n(\phi) = \left(\frac{\partial^2 \log L}{\partial \phi \, \partial \phi^T}\right)$. Using the large sample approximation, MLE of ϕ, i.e $\hat{\phi}$ can be approximated by $N_2(\phi; V_n(\phi)^{-1})$, where $V_n(\phi) = E[U_n(\phi)]$. When certain requirements are met for parameters located within the parameter space but not on its boundary, the asymptotic distribution of $\sqrt{n}(\hat{\phi} - \phi)$ is $N_2(\phi; V_n(\phi)^{-1})$, where $V(\phi) = \lim_{n\to\infty} n^{-1}U_n(\phi)$ is taken to be the unit information matrix. This asymptotic tendency is true even

if $V(\phi)$ is substituted with the mean sample information matrix that is assessed at $\hat{\phi}$, say $n^{-1}U_n(\hat{\phi})$. The estimated asymptotic multivariate normal $N_2(\phi; V_n(\hat{\phi})^{-1})$ distribution of $\hat{\phi}$ can be utilized to construct approximate confidence intervals for the parameters of the distribution. A $100(1 - \varepsilon)$ asymptotic confidence interval for each parameter ϕ_q is given by

$$ACI_q = \left(\hat{\phi}_q - Z_{n/2}\sqrt{\hat{U}_{qq}}, \hat{\phi}_q + Z_{n/2}\sqrt{\hat{U}_{qq}} \right).$$

where $\hat{U}_{qq}$ is the (q, q) diagonal element of $V_n(\hat{\phi})^{-1}$ for $q = 1, 2$, and $Z_{n/2}$ is the quantile $1 - {}^n/_2$ of the standard normal distribution.

5 | Simulation Study

Simulations were carried out to assess the effectiveness of the proposed method of MLE procedure in estimating the parameters of the IRG distribution. The random number generation for the study was performed based on 1000 samples of size 20, 50, 80, and 150, each of which was randomly sampled using the inversion method based on the QF given in *Eq. (12)*. The process was repeated 1000 times to derive the following:

$$\text{Absolute Bias } (|AB|) = \frac{1}{M}\sum_{i=1}^{M} |\hat{\phi}_i - \phi|.$$

$$\text{Mean Squared Error (MSE)} = \frac{1}{M}\sum_{i=1}^{M} \left(\hat{\phi}_i - \phi\right)^2.$$

These are given in *Tables 4-6*. We discover that the mean square error approaches zero as the sample size increases, as expected, which indicates that maximum likelihood performed consistently.

Table 4. Estimates, squared error, and mean squared errors of inverse Rayleigh geometric distribution for maximum likelihood estimations by using different parameter values ($\rho = 0.5$, $v = 0.5$).

n	Parameter	Mean	(AB)	SE	MSE
20	ρ	0.3811	0.1189	0.1467	0.0357
	v	0.7165	0.2165	0.2152	0.0932
50	ρ	0.4092	0.0908	0.0790	0.0145
	v	0.3632	0.1368	0.2375	0.0751
80	ρ	0.5316	0.0316	0.0973	0.0105
	v	0.4822	0.0178	0.1974	0.0393
100	ρ	0.5284	0.0284	0.0869	0.0084
	v	0.4676	0.0324	0.1806	0.0337
150	ρ	0.5392	0.0392	0.0693	0.0063
	v	0.5569	0.0569	0.1226	0.0183

Table 5. Estimates, squared error, and mean squared errors of inverse Rayleigh geometric distribution for maximum likelihood estimations by using different parameter values ($\rho = 1.3$, $v = 0.5$).

n	Parameter	Mean	(AB)	SE	MSE
20	ρ	1.2583	0.0417	0.3828	0.1483
	v	0.7197	0.2197	0.2132	0.0937
50	ρ	1.5815	0.2815	0.3415	0.1959
	v	0.6059	0.1059	0.1874	0.0463
80	ρ	1.3892	0.0892	0.2513	0.0711
	v	0.4891	0.0109	0.1923	0.0371
100	ρ	1.3796	0.0796	0.2260	0.0574
	v	0.4718	0.0282	0.1789	0.0328
150	ρ	1.3027	0.0027	0.1782	0.0318
	v	0.5102	0.0102	0.1200	0.0145

Table 6. Estimates, squared error, and mean squared errors of inverse Rayleigh geometric distribution for maximum likelihood estimations by using different parameter values ($\rho = 0.5$, $v = 0.8$).

n	Parameter	Mean	(AB)	SE	MSE
20	ρ	1.4156	0.0844	0.3603	0.1369
	v	0.8791	0.0791	0.0940	0.0151
50	ρ	1.1964	0.3036	0.2345	0.1472
	v	0.7232	0.0768	0.1297	0.0440
80	ρ	1.2939	0.2061	0.1951	0.0805
	v	0.7517	0.0483	0.0919	0.0108
100	ρ	1.3580	0.1420	0.1821	0.0533
	v	0.7516	0.0484	0.0868	0.0099
150	ρ	1.4449	0.0001	0.1534	0.0235
	v	0.7955	0.0045	0.0562	0.0032

6|Applications of Inverse Rayleigh Geometric to Lifetime Data Sets

In this section, we demonstrate three lifetime data applications of the proposed model in which two of the data sets follow a monotonic failure rate and one follows a non-monotonic failure rate, so as to achieve the primary objectives of extending the IR model. The performance of the models considered is judged using certain information criteria commonly used to evaluate the goodness of fit measures, which are Akaike Information Criterion (AICr), Bayesian Information Criterion (BICr), and Consistent Akaike Information Criterion (CAICr), Kolmogorov-Smirnov (KS), and the Probability Value (PV) are calculated to compare the fitted models. The model with the smallest values of these measures with the highest probability value is judged to be better than the others. These criteria are mathematically represented as follows:

$$\text{AICr} = -2l + 2h, \quad \text{AICr} = \text{AICr} + \frac{2h(h + 1)}{n - h - 1},$$

$$\text{CAICr} = -2L + h\{\log(n) + 1\},$$

$$\text{BICr} = h\log(n) - 2L, \qquad \text{HQICr} = -2L + 2h\log\{\log(n)\},$$

where, $L = L(\hat{\phi}; z_i)$ represent the Maximized Likelihood (ML) function and z_i is the given random sample, $\hat{\phi}$ is the ML estimator and h is the number of parameter(s) in the model.

The first data set consists of 63 observations of the strengths of 1.5 cm glass fibers obtained by workers at the UK National Physical Laboratory. The data have been previously analysed by Ogunde et al. [31], Reyad et al. [32] and Merovci et al. [33]. The summary statistics of the data are given in *Table 7*, which show that the data is negatively skewed, leptokurtic with excess Kurtosis of 0.9, and under-dispersed. The total time on test (TTT) plot, the Violin plot, and the Box plot are given in *Fig. 6*, which shows that the data is negatively skewed
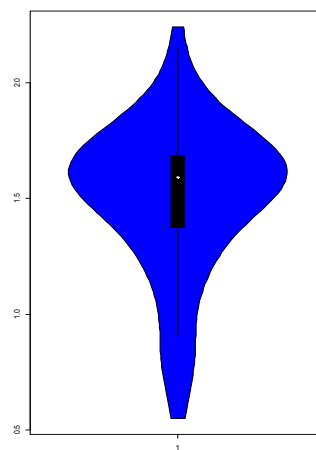
with an increasing failure rate. The MLEs' estimates of the parameters of the models considered are given in *Table 8*.

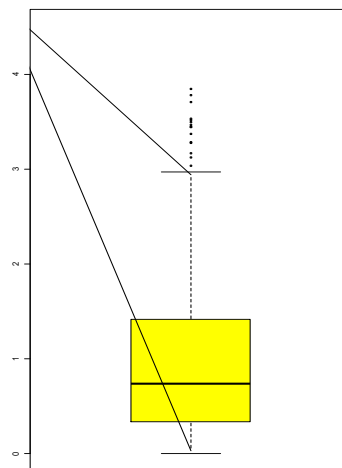**Table 7. Summary statistics for the first data set.**

q₁	Median	Mean	q₃	Range	Variance	Kurtosis	Skewness
1.38	1.59	1.51	1.69	1.69	0.11	3.92	-0.89

a.

b.

c.
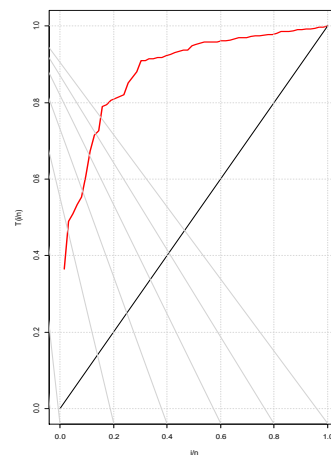
Fig. 7. a. Total time on test plot, b.Violin density for the first data, and c. Box plot for the first data.

Table 8. Maximum likelihood estimations, standard errors (in parentheses), and Goodness-of-fit statistics for the first data set.

Model	Parameters Estimates		Measures of Goodness of Fit						
	ρ	v	$-l$	AICr	BICr	CAICr	HQICr	KS	PV
GIRG	4.34 (0.78)	0.84 (0.07)	46.64	97.27	101.56	97.47	98.96	0.2294	0.0026
IW	1.97 (0.24)	2.89 (0.23)	46.85	97.70	101.99	97.91	99.39	0.2434	0.0011
IL	19.61 (14.15)	28.38 (20.56)	90.44	184.88	189.17	185.08	186.57	0.4932	9.8e-14
L	14.07 (7.11)	21.42 (11.18)	90.91	185.81	190.10	186.01	187.50	0.4070	1.7e-09
EIR	0.69 (5.96)	2.56 (21.92)	54.7	113.3	117.6	113.5	115.0	0.3472	5.01e-07
IR	1.70 (0.23)	- (-)	54.66	111.31	113.45	111.38	112.15	0.3472	5.1e-07

The IRG distribution is the best-fitted model among the other competing models considered in this study because the values of all criteria of goodness of fit are significantly smaller for the IRG distribution. The LR statistic was obtained for testing the hypotheses $H_0: v = 1$ 1versus $H_1 = H_0$ It is not true to compare the IR model with the IRG model. The LR statistic $G = 2\{-46.64 - (-54.66)\} = 16.04$ (p − value < 0.01), which is sufficient to show that the IRG model is a better model that can be used in fitting the data than the IR model.

The second data set is from Bjerkedal [34] and represents the survival times, in days, of guinea pigs injected with different doses of tubercle bacilli. The data set consists of 72 observations. The data have been previously analysed by Ogunde and Adeniji [35]. The summary statistics of the data are given in *Table 9*, which show that the data is positively skewed, mesokurtic with excess Kurtosis of −1.2, and over-dispersed. The TTT plot, Violin plot, and the Box plot are given in *Fig. 7*, which shows that the data is positively skewed with a non-monotonic failure rate. The MLEs' estimates of the parameters of the models considered are given in *Table 10*.
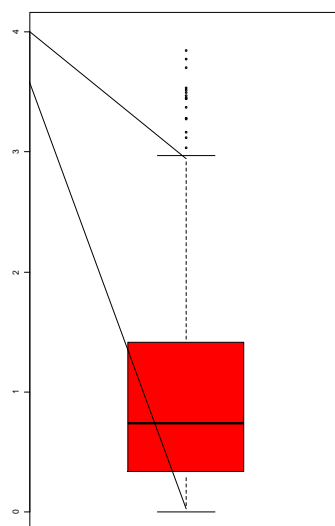
Table 9. Summary statistics for the second data set.

| q_1	Median	Mean	q_3	Range	Variance	Kurtosis	Skewness
54.75	70	99.82	112.75	364	6580.12	5.61	1.80

a.

b.

c.
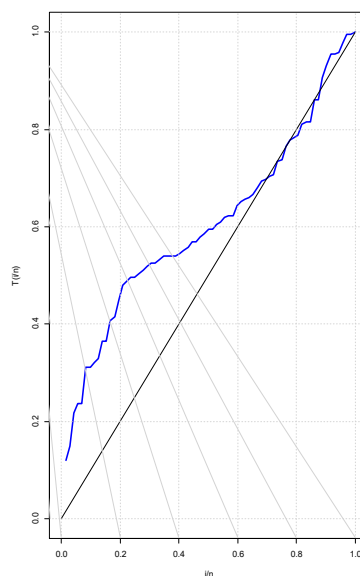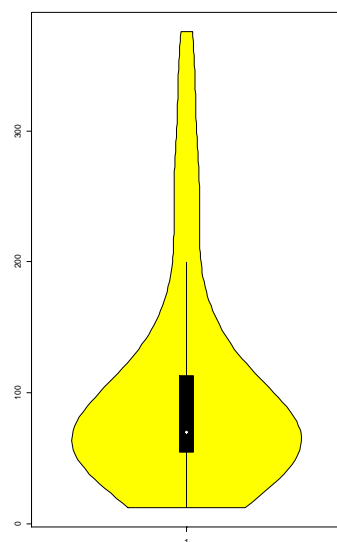
Fig. 7. a. Total time on test plot, b. Violin density for the
second data, and c. Box plot for the second data set.

Table 10. Maximum likelihood estimations, standard errors (in parentheses), and Goodness-of-fit
**statistics for the second data set.**

Model	Parameters Estimates		Measures of Goodness of Fit						
	ρ	v	-l	AICr	BICr	CAIC	HQICr	KS	PV
GIRG	58.62 (12.32)	-57.53 (12.40)	395.69	795.38	799.93	795.55	797.19	0.2436	0.0004
IW	20.84 (4.45)	0.78 (0.06)	414.89	833.77	838.32	833.94	835.58	0.1951	0.0083
IL	0.09 (0.04)	6.51 (2.70)	405.20	814.38	818.94	814.56	816.20	0.2134	0.0028
L	0.89 (0.15)	39.76 (8.81)	427.50	859.0	863.55	859.17	860.81	0.3397	1.21e-07
EIR	50.35 (15.73)	43.42 (13.75)	406.7	817.5	822.0	817.7	819.3	0.2511	0.0002
GIR	0.60 (0.08)	0.03 (0.01)	400.9	805.9	810.4	806.0	807.7	0.9999	2.2e-16
IR	78.67 (9.27)	- (-)	576.8	1155.5	1157.8	1155.6	1156.42	0.8566	2.2e-16

The IRG distribution is the best-fitted model among the other competing models considered in this study because the values of all criteria of goodness of fit are significantly smaller for the IRG distribution. The LR statistic was obtained for testing the hypotheses $H_0: v = 1$ versus $H_1 = H_0$ is not true that the IR model is

compared with the IRG model. The LR statistic $G = 2\{-395.69 - (-576.80)\} = 362.22$ (p $-$ value $<$ 0.01), which is sufficient to show that the IRG model is a better model that can be used in fitting the data than the IR model.
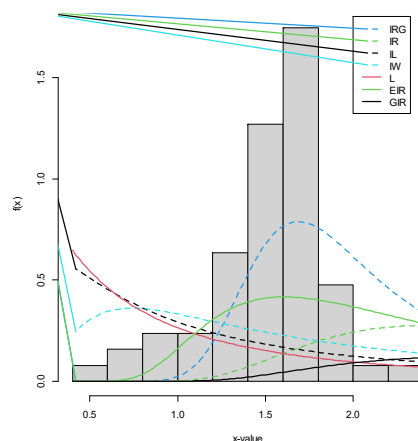
a.
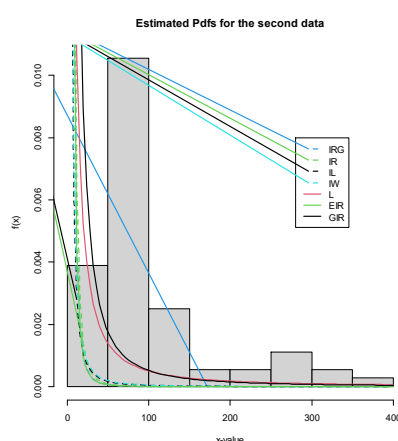
b.

Fig. 8. Fitted densities for the inverse Rayleigh geometric distribution; a. Estimated probability density functions first data, and b. Estimated probability density functions for the second data.

7 | Conclusion

In this work, we have proposed and derived the properties and applications of the IRG distribution. The model extends the well-known IR distribution by the addition of one parameter. We derived an explicit mathematical expression for the moments, incomplete moments, MGF, weighted moment, stress-strength reliability, Bonferroni and Lorenz curves, mean deviations, residual life, reversed residual life functions, order statistics, Rényi, and Tsallis entropies. We estimated the model parameters using the method of maximum likelihood and determined their applicability using simulation studies. Finally, we fit the model to two lifetime data set to demonstrate its applicability and flexibility; the results demonstrate that the IRG model provides a better fit than some other popularly used reliability models as measured regarding the AICr, BICr, CAICr, KS, and PV, which is also adequately supported the fitted densities in *Fig. 8*. We hope that this distribution will attract wider applications in the areas of sciences and applied sciences

References

[1] Trayer, V. N. (1964). Inverse rayleigh (IR) model. *Proceedings of the academy of science, doklady akad, nauk belarus, ussr*. Izd-vo Akademii nauk BSSR.

[2] Voda. (1972). On the inverse Rayleigh distributed random variable. *Reports of statistical application and research of the union of Japanese scientists and engineers*, *19*(4), 13–21.

[3] Gharraph, M. K. (1993). Comparison of estimators of location measures of an inverse Rayleigh distribution. *The Egyptian statistical journal*, *37*(2), 295–309. https://doi.org/10.21608/esju.1993.426926

[4] Mukherjee, S. P., & Maiti, S. S. (1996). A percentile estimator of the inverse Rayleigh parameter. *IAPqR transactions*, *21*, 63–66.

[5] Soliman, A., Amin, E. A., & Abd-El Aziz, A. A. (2010). Estimation and prediction from inverse Rayleigh distribution based on lower record values. *Applied mathematical sciences*, *4*(62), 3057–3066. https://m-hikari.com/ams/ams-2010-ams-61-64-2010/aminAMS61-64-2010.pdf

[6] Almarashi, A. M., Badr, M. M., Elgarhy, M., Jamal, F., & Chesneau, C. (2020). Statistical inference of the half-logistic inverse Rayleigh distribution. *Entropy*, *22*(4). https://doi.org/10.3390/e22040449

[7] Chiodo, E., & Noia, L. P. Di. (2020). Stochastic extreme wind speed modeling and bayes estimation under the inverse Rayleigh distribution. *Applied sciences*, *10*(16). https://doi.org/10.3390/app10165643

[8] Chiodo, E., Fantauzzi, M., & Mazzanti, G. (2022). The compound inverse Rayleigh as an extreme wind speed distribution and its bayes estimation. *Energies*, *15*(3). https://doi.org/10.3390/en15030861

[9] Bakoban, R. A., & Al-Shehri, A. M. (2021). A new generalization of the generalized inverse Rayleigh distribution with applications. *Symmetry*, *13*(4). https://doi.org/10.3390/sym13040711

[10] Khan, M. S. (2014). Modified inverse Rayleigh distribution. *International journal of computer applications*, *87*(13), 28–33. https://core.ac.uk/download/pdf/33703289.pdf

[11] Khan, M. S., & King, R. (2015). Transmuted modified inverse Rayleigh distribution. *Austrian journal of statistics*, *44*(3), 17–29. http://dx.doi.org/10.17713/ajs.v44i3.21

[12] Goual, H., & Yousof, H. M. (2020). Validation of Burr XII inverse Rayleigh model via a modified chi-squared goodness-of-fit test. *Journal of applied statistics*, *47*(3), 393–423. https://doi.org/10.1080/02664763.2019.1639642

[13] Fatima, K., & Ahmad, S. P. (2017). Weighted inverse Rayleigh distribution. *International journal of statistics and systems*, *12*(1), 119–137. https://b2n.ir/zp9182

[14] Rao, G. S., & Mbwambo, S. (2019). Exponentiated inverse Rayleigh distribution and an application to coating weights of iron sheets data. *Journal of probability and statistics*, *2019*(1), 7519429. https://doi.org/10.1155/2019/7519429

[15] Banerjee, P., & Bhunia, S. (2022). Exponential transformed inverse rayleigh distribution: Statistical properties and different methods of estimation. *Austrian journal of statistics*, *51*(4), 60–75. https://doi.org/10.17713/ajs.v51i4.1338

[16] Marshall, A. W., & Olkin, I. (1997). A new method for adding a parameter to a family of distributions with application to the exponential and Weibull families. *Biometrika*, *84*(3), 641–652. https://doi.org/10.1093/biomet/84.3.641

[17] Eugene, N., Lee, C., & Famoye, F. (2002). Beta-normal distribution and its applications. *Communications in statistics-theory and methods*, *31*(4), 497–512. https://doi.org/10.1081/STA-120003130

[18] Cordeiro, G. M., & de Castro, M. (2011). A new family of generalized distributions. *Journal of statistical computation and simulation*, *81*(7), 883–898. https://doi.org/10.1080/00949650903530745

[19] Alexander, C., Cordeiro, G. M., Ortega, E. M. M., & Sarabia, J. M. (2012). Generalized beta-generated distributions. *Computational statistics & data analysis& data analysis*, *56*(6), 1880–1897. https://doi.org/10.1016/j.csda.2011.11.015

[20] Shaw, W. T., & Buckley, I. R. C. (2009). *The alchemy of probability distributions: Beyond Gram-Charlier expansions, and a skew-kurtotic-normal distribution from a rank transmutation map*. https://doi.org/10.48550/arXiv.0901.0434

245

Ogunde et al. | Ann. Proc. Eng. Manag. 2(4) (2025) 225-245

[21] Elgarhy, M., Arslan Nasir, M., Jamal, F., & Ozel, G. (2018). The type II Topp-Leone generated family of distributions : Properties and applications. *Journal of statistics and management systems*, *21*(8), 1529–1551. https://doi.org/10.1080/09720510.2018.1516725

[22] Alzaatreh, A., & Ghosh, I. (2015). On the Weibull-X family of distributions. *Journal of statistical theory and applications*, *14*(2), 169–183. https://doi.org/10.2991/jsta.2015.14.2.5

[23] Tahir, M. H., Cordeiro, G. M., Alizadeh, M., Mansoor, M., Zubair, M., & Hamedani, G. G. (2015). The odd generalized exponential family of distributions with applications. *Journal of statistical distributions and applications*, *2*(1), 1–28. https://doi.org/10.1186/s40488-014-0024-2

[24] Muhammad, M. (2016). Poisson-odd generalized exponential family of distributions: Theory and applications. *Hacettepe journal of mathematics and statistics*, *47*(6), 1652–1670. https://dergipark.org.tr/en/download/article-file/594135

[25] Yousof, H. M., Afify, A., Alizadeh, M., Hamedani, G., Amir Jahanshahi, S. M., & Ghosh, D. I. (2018). The Generalized Transmuted Poisson-G Family of Distributions: Theory, Characterizations and Applications. *Pakistan journal of statistics and operation research*, *14*(4), 759–779. https://doi.org/10.18187/pjsor.v14i4.2527

[26] Chesneau, C., & Jamal, F. (2021). The sine Kumaraswamy-G family of distributions. *Journal of mathematical extension*, *15*(2), 1–33. ttps://doi.org/10.30495/JME.2021.1332

[27] Al-Babtain, A. A., Elbatal, I., Chesneau, C., & Elgarhy, M. (2020). Sine Topp-Leone-G family of distributions: Theory and applications. *Open physics*, *18*(1), 574–593. https://doi.org/10.1515/phys-2020-0180

[28] Galton, F. (1883). *Inquiries into human faculty and its development*. Macmillan. https://B2n.ir/ts3472

[29] Moors, J. J. A. (1988). A quantile alternative for kurtosis. *Journal of the royal statistical society: Series d (the statistician)*, *37*(1), 25–32. https://doi.org/10.2307/2348376

[30] Tsallis, C. (1988). Possible generalization of Boltzmann-Gibbs statistics. *Journal of statistical physics*, *52*(1), 479–487. https://doi.org/10.1007/BF01016429

[31] Ogunde, A. A., Laoye, V. E., Ezichi, O. N., & Balogun, K. O. (2021). Harris extended power Lomax distribution: Properties, inference and applications. *International journal of statistics and probability*, *10*(4), 77–95. https://doi.org/10.5539/ijsp.v10n4p77

[32] Reyad, H. M., & Othman, S. A. (2017). The beta compound Rayleigh distribution: Properties and applications. *Int. j. adv. stat. prob*, *5*(1), 57–64. https://doi.org/10.14419/ijasp.v5i1.7513

[33] Merovci, F., Khaleel, M. A., Ibrahim, N. A., & Shitan, M. (2016). The beta Burr type X distribution properties with application. *SpringerPlus*, *5*(1), 697. https://doi.org/10.1186/s40064-016-2271-9

[34] Bjerkedal, T. (1960). Acquisition of resistance in guinea pies infected with different doses of virulent tubercle bacilli. *American journal of hygiene*, *72*(1), 130–148. https://doi.org/10.5555/19612700619

[35] Ade Ogunde, A., & Adeniji, O. E. (2022). Type II Topp-Leone Bur XII distribution: Properties and applications to failure time data. *Scientific African*, *16*, e01200. https://doi.org/10.1016/j.sciaf.2022.e01200